Applied Physics B manuscript No.
(will be inserted by the editor)

Efficient two-stage dual-beam noncollinear optical parametric amplifier

Yu-Hsiang Cheng[1], Frank Y. Gao[2], Peter R. Poulin[2], Keith A. Nelson[2]

[1] Department of Electrical Engineering and Computer Science, Massachusetts Institute of Technology, Cambridge, Massachusetts, 02139 (Phone: +1-6172531956, Fax: +1-6172587500, E-mail: yuhsiang@mit.edu)
[2] Department of Chemistry, Massachusetts Institute of Technology, Cambridge, Massachusetts, 02139

Received: date / Revised version: date

Abstract We have constructed a noncollinear optical parametric amplifier with two signal beams amplified in the same nonlinear crystal. This dual-beam design is more energy-efficient than operating two amplifiers in parallel. The cross-talk between two beams has been characterized and discussed. We have also added a second amplification stage to enhance the output of one of the arms, which is then frequency-doubled for ultraviolet generation. This single device provides two tunable sources for ultrafast spectroscopy in the ultraviolet and visible region.

1 Introduction

Having multiple beams with tunable wavelengths in the visible is invaluable for many spectroscopic applications related to electronic or vibrational resonances such as resonance-enhanced Raman scattering, transient absorption, and femtosecond photochemistry. As the wavelength of a laser oscillator is only narrowly tunable, a common way to generate tunable sources is the optical parametric process, a second-order nonlinear effect. The first optical parametric oscillator was demonstrated in 1965 [1]. In a collinear geometry, the phase-matching condition limits the gain bandwidth yielding output pulses in the visible often longer than 30 fs [2]. To match the group velocity of the signal and idler pulses, a noncollinear geometry has been applied to optical parametric oscillators [3,4] and amplifiers [5,6]. Pumped by the second harmonic of a Ti:sapphire laser, phase-matching in a β-BaB_2O_4 (BBO) crystal can be simultaneously satisfied for signal wavelengths between 480 nm and 790 nm and pulses as short as 4 fs have been generated from a noncollinear optical parametric amplifier (NOPA) [7]. At a 1 kHz repetition rate, the pulse energy from a single-stage NOPA is usually a few µJ but can be further boosted up to 300 µJ with a second amplification stage [8]. After more than 20 years of development, NOPAs have become a common tool for ultrafast spectroscopy laboratories. More reviews about NOPAs can be found in references [9–12].

As we demonstrate in this paper, another benefit of the noncollinear configuration is the ability to amplify multiple signal beams in a single nonlinear crystal with the same pump pulse, which is simpler, more compact, and more energy-efficient than constructing multiple NOPAs in parallel. This design can also be readily adapted for use in many existing NOPA setups at a small cost to the overall performance characteristics. Our dual-beam NOPA offers two tunable visible pulses with phase coherence, which are particularly useful for ultrafast pump-probe spectroscopy or two-dimensional spectroscopy. To access transitions with higher energies, we further amplify one of the visible pulses by a second amplification stage and double its frequency to generate tunable ultraviolet light. A variety of electronic resonances can be studied with the two tunable visible-ultraviolet sources, generated by a single NOPA.

2 Two-stage dual-beam NOPA

A schematic of the experimental setup is shown in Fig. 1. The light source was a commercial Ti:sapphire regenerative amplifier system with a central wavelength of 800 nm, which produced 60-fs pulses with 1.6 mJ energy at a repetition rate of 1 kHz. The majority of the laser energy was sent into a 300-µm-thick BBO crystal (θ=29°) for type I second harmonic generation (o+o→e). A conversion efficiency higher than 40% was achieved though the spatial beam quality of the second harmonic was degraded. If a better spatial mode is desired, the conversion efficiency should be set lower than 30% [8]. The second harmonic beam with 600 µJ pulse energy was then separated by a 10:90 beam splitter to pump the two stages. No compression of the pump was necessary, as the temporally stretched pump yielded more bandwidth when amplifying the highly chirped seed.

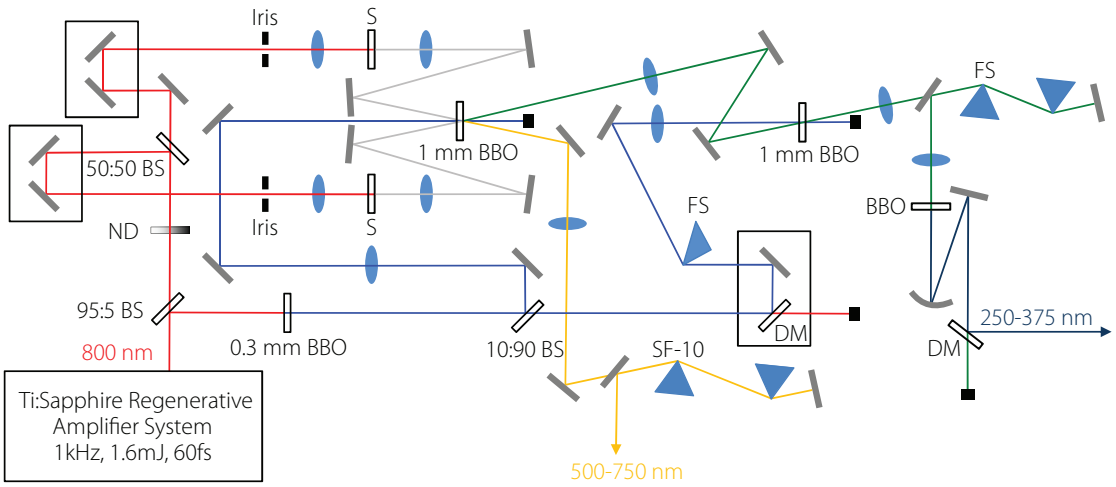

Fig. 1 Schematic illustration of the two-stage dual-beam NOPA setup. BS, beamsplitter; ND, neutral-density filter; S, sapphire plate; FS, fused silica; DM, dielectric mirror for ultraviolet wavelengths.

A small portion of the laser energy ∼1 µJ was focused in a 2-mm-thick sapphire plate to generate single-filament white-light continuum, spanning from 0.45 µm to 1.2 µm [13–15]. After optimizing the pulse energy with a variable attenuator and the numerical aperture with an iris, a stable white-light pulse with a nearly Gaussian beam shape was generated. The RMS fluctuations were about 0.5%, measured after a shortpass filter cut off at 750 nm. We suggest monitoring the fluctuation while optimizing the white-light generation. In our dual-beam NOPA, two white-light seeds were generated separately and sent into the same BBO crystal as signal pulses. To make this device even more compact, one can generate a single white-light seed and then split it into two beams [16], though the chirp of the two seeds might become unequal due to a beam splitter.

In the first NOPA stage, the 400-nm pump amplified the white-light seed via a Type I optical parametric process (e→o+o) in a 1-mm-thick BBO crystal (θ=31°), whose thickness was limited by the separation between the pump and signal pulses due to group velocity dispersion. The pump was focused in front of the BBO crystal to compensate for self-focusing effects [13] and its intensity at the crystal could be optimized by translating the focusing lens. Without seed pulses, a visible parametric superfluorescence cone with a ∼6° external apex angle (∼3.6° internal angle) was generated and served as a guide to align the white-light seeds. Once the pump and seed overlapped temporally and spatially, and the phase-matching condition was satisfied, the signal beam was amplified and an idler beam was generated.

For our own applications (single-shot spectroscopy [17]), relatively narrowband pulses were preferred so we chose a singlet lens rather than a curved mirror to focus the white light. In this case, the group delay dispersion and the chromatic aberration of the lens limited the usable bandwidth. As the white-light seed was strongly chirped, the wavelength to be amplified could be easily tuned by adjusting the temporal overlap of the pump and seed via a delay stage. The conversion efficiency of a NOPA for these narrowband pulses is similar to that in the broadband case. However, due to chromatic aberration, the position of the singlet lens needed to be adjusted to match the pump size when switching between wavelengths. Achromatic doublet lenses could be used instead but the bandwidth would be further reduced. If shorter pulse widths are desired, focusing by reflective optics, pre-compression of the seed, or pre-chirping of the pump can be applied [10].

The signal could be tuned between 500 and 750 nm as limited by idler absorption and signal-pump group-velocity mismatch [18]. We found the maximal pulse energy to be 10 µJ at 510 nm, corresponding to a 21% conversion efficiency with RMS fluctuations of 1.5%. The amplified signal beam was then compressed by a pair of SF-10 prisms with a tip-tip spacing of 25 cm or fused silica prisms with a spacing of 70 cm, yielding pulses as short as 26 fs. To reduce higher-order phase distortions, the beam is passed near the tip of the prisms. The loss of the compressor was about 10%. For better compression, chirped mirrors [19] or adaptive optics [10,20] can be used. The pulse width was measured by second-harmonic-generation frequency-resolved optical gating with a 20-µm-thick BBO crystal [21]. The spectra are shown in Fig. 2 and the performance of the NOPA is summarized in Table 1.

The seed can be amplified as long as it is an ordinary ray propagating along the direction of the fluorescence cone (and overlapping with the pump beam). Therefore, multiple signal beams can be amplified in a single NOPA. Idler beams are generally emitted at a larger angle and will not mix with the signal beams. In our dual-beam NOPA design, the two beams can be tuned almost independently and can be applied to two-color experiments in the visible region. The competition between two beams for pump power becomes more obvi-

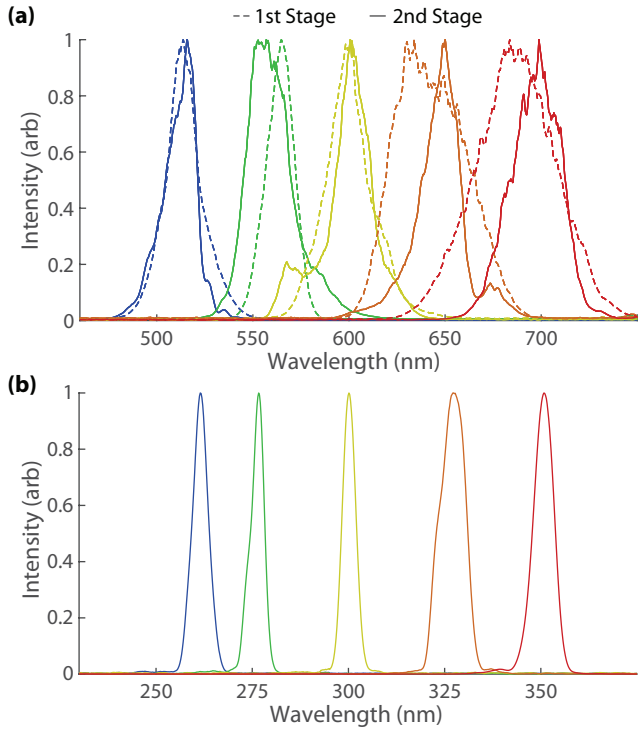

Fig. 2 Normalized spectra of (a) tunable visible pulses from the two NOPA stages and (b) the ultraviolet pulses generated in a 20-µm-thick BBO crystal.

Table 1 Summary of the performance of the two-stage NOPA. Pulse energies were measured before compression with one-beam amplification in the first stage.

λ (nm)	Bandwidth (nm)	Pulse width (fs)	Energy (μJ)
First stage, 48 µJ pump			
510	17	33	10
550	16	32	6
600	25	29	3
650	46	28	2.4
700	47	26	1.8
Second stage, 410 µJ pump			
510	17	31	106
550	25	22	70
600	19	30	68
650	20	29	51
700	29	32	36

ous when the conversion efficiency is high and pump depletion becomes important. With dual beams, the pulse energy of each beam is 8 µJ at 510 nm instead of 10 µJ. Thus, the maximum pump-to-signal conversion efficiency of each beam dropped by 4% but the combined efficiency increased to 33%. If we further include the idler energy, the total conversion efficiency became 42%. This high conversion efficiency will be highly desired for low-power or high-repetition-rate lasers.

Since the parametric process depends on the pump intensity, fluctuations in one branch will lead to different degrees of pump depletion and will thus induce effects in the other branch. We analyze the cross-talk between two beams carefully and this is summarized in Fig. 3. First, the output energies of the two amplified beams were correlated not only due to the energy fluctuations of the fundamental laser (positive correlation) but also due to the competition for pump energy (negative correlation). To examine such correlations closely, we attenuated one white-light seed by a variable neutral-density filter to control the degree of pump depletion and measured the change in pulse energy and RMS fluctuations of the other beam. As the degree of pump depletion increased, the pulse energy of the unattenuated beam decreased from 10 µJ to 8 µJ and the RMS fluctuations increased from 0.8% to 1.5%. For practical applications, we believe the fluctuations are still tolerable, especially with standard chopping or balancing techniques. The second phenomenon we observed when another beam was inserted was a minor modification in the beam shape (size) and propagation direction due to a Kerr lens effect in the BBO crystal. As the pump intensity decreases due to the insertion of a second beam, the Kerr lens effect is reduced and the propagation of the original beam is slightly deflected. However, we did not observe an obvious increase of pointing fluctuations of either beam. We believe the Kerr lensing will not be an issue as long as one is not chopping one of white-light seeds before amplification. Third, we did not observe a significant change in the spectrum or the compressed pulse width induced by the insertion of another seed, as any changes seen were within our experimental error. Lastly, we want to comment on the phase coherence of the two beams. Since the white-light seeds generated from the same laser source were phase-locked [22] and the parametric amplification preserves this phase relation [16], the two amplified signals should be phase coherent. When the two beams were overlapped in time and space, a fringe pattern from the resulting interference was clearly seen so we believe the extra phase jitter induced by the cross-talk was small. Note that one can try to avoid the cross-talk discussed above by increasing the pump beam size or the pump pulse duration so that two beams overlap with different parts of the pump spatially or temporally, though doing so will decrease the conversion efficiency.

As higher pulse energies were desired for ultraviolet generation, an additional amplification was added. However, to utilize the higher pump power, the beam size at the BBO crystal had to be large enough that the spatial chirp due to pulse front mismatch became problematic [8,10]. As such, the pump wavefront was tilted by 2.3° after passing through a fused-silica right-angle prism with an incident angle of 34° [23]. The pump beam was then focused behind the BBO crystal to shrink the beam size at the crystal and match its wavefront with the seed wavefront. We did not focus the beam in front of the BBO crystal in order to avoid plasma generation in air. As the tilted pulse front increased the interaction length and the overlap between pulses, the beam spatial

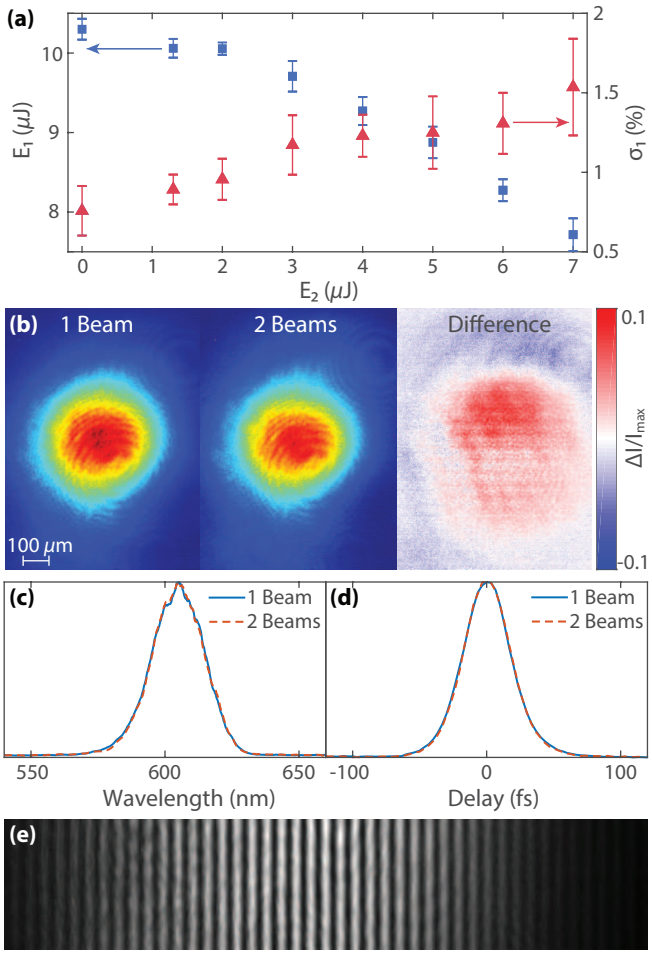

Fig. 3 (a) The pulse energy E_1 and RMS fluctuations σ_1 of one beam while attenuating the pulse energy E_2 of the other beam. Both beams were at 510 nm. (b) The beam profile of one signal beam in the first stage with and without another signal beam, measured 36 cm away from the BBO crystal. The ring patterns were artifact. (c) The spectrum and (d) the intensity autocorrelation of one signal beam with and without another beam. (e) The interference pattern when two signal beams overlap.

profile, the compressed pulse width, and the conversion efficiency were all considerably improved. However, because the wavefront tilt also results in an asymmetric superfluorescence ring, a dual-beam design is not suitable in the second stage. After the second amplification stage, the maximal pulse energy was 106 µJ at 510 nm and RMS fluctuations were about 1.2% with single-beam amplification in the first stage. The pulse energy became 93 µJ with RMS fluctuations of 1.5% when both beams were amplified in the first stage. The spectrum and the pulse width after compression were nearly unchanged by the additional beam in the first stage. We sometimes detuned the central wavelengths of the two stages to achieve a better compression with minimal effects on the conversion efficiency.

To generate ultraviolet pulses, the output beam from the second amplification stage was then focused into a BBO crystal for type-I second harmonic generation. The ultraviolet output was generally tunable between 250 and 375 nm, and the spectra are shown in Fig. 2. Since the phase-matching angle and the group velocity mismatch between the visible and ultraviolet pulses strongly depend on the wavelength, the BBO orientation and thickness need to be optimized for each wavelength to avoid lengthening the ultraviolet pulses. When generating pulses at 265 nm in a 100-µm-thick BBO crystal, the pulse energy was 7 µJ and the pulse duration was about 100 fs. With a 20-µm-thick BBO crystal (with the fused silica substrate of the BBO crystal facing the incoming beam), the pulsewidth was reduced to 35 fs. For pulses at 300 nm generated in a 100-µm-thick BBO crystal, the pulse energy was about 3 µJ and the pulse duration was 66 fs. The pulsewidth of the ultraviolet pulses was measured using an autocorrelator based on two-photon absorption in a 100-µm-thick BBO crystal [24]. If the uncompressed visible pulse is sufficiently short, one can move the compressor after the ultraviolet generation to have better control of dispersion in the ultraviolet spectral domain [25]. Furthermore, instead of frequency doubling, one can also frequency sum the NOPA output with 800-nm pulses to generate stronger ultraviolet pulses with a narrower tuning range [26].

3 Applications

In order to demonstrate the practical applications of this two-stage dual-beam NOPA, we have conducted single-shot pump-probe measurements in a triiodide (I_3^-) solution using 300-nm pump and 600-nm probe pulses, as shown in Fig 4. Absorption of the pump pulse photodissociates I_3^- forming atomic iodine and a diiodide ion (I_2^-), the latter of which absorbs the probe beam [27]. After a delay about 300 fs, the coherent oscillations of I_2^- are clearly seen. A single-stage dual-beam NOPA with reflective optics (shortest pulsewidth about 10.6 fs) has previously been realized in our group [28] and successfully applied to ultrafast spectroscopy using an ultraviolet pump and a visible probe [29].

4 Conclusions

In summary, we demonstrate the novel design of a dual-beam NOPA, a straight-forward, energy efficient, and relatively easy to build extension to an existing one-or-two stage NOPA which can output an additional tunable beam with only a relatively minor effect on the noise and power characteristics of either beams. Powered by 1.6-mJ 800-nm pulses, the output of our NOPA was tunable from 500 to 750 nm with pulse energies up to 10 µJ for the first stage and 106 µJ for the second stage. Tunable ultraviolet pulses were also generated via frequency doubling. This dual-beam source is useful for ultrafast spectroscopy in the visible and ultraviolet regions

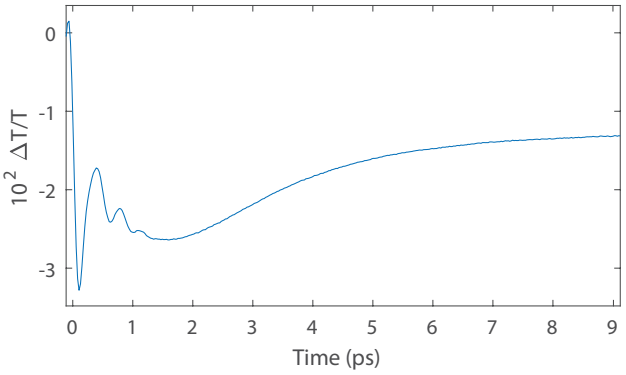

Fig. 4 Transient absorption of triiodide in ethanol solution with a pump wavelength at 300 nm and a probe wavelength at 600 nm.

and its high conversion efficiency is especially valuable for applications utilizing low-power or high-repetition-rate lasers. It is also valuable for measurements requiring phase-coherent pulses at widely varying frequencies such as multi-dimensional spectroscopy.

Acknowledgements The authors want to thank Andreas Steinbacher for many useful discussions. This work was supported by National Science Foundation Grants No. 1665383 and by Office of Naval Research Grant No. N00014-12-1-0530.

References

1. J. A. Giordmaine and R. C. Miller, Phys. Rev. Lett. **14**, 973 (1965).
2. M. K. Reed, M. S. Armas, M. K. Steiner-Shepard, and D. K. Negus, Opt. Lett. **20**, 605 (1995).
3. T. J. Driscoll, G. M. Gale, and F. Hache, Opt. Commun. **110**, 638 (1994).
4. G. M. Gale, M. Cavallari, T. J. Driscoll, and F. Hache, Opt. Lett. **20**, 1562 (1995).
5. P. Di Trapani, A. Andreoni, C. Solcia, P. Foggi, R. Danielius, A. Dubietis, and A. Piskarskas, J. Opt. Soc. Am. B **12**, 2237 (1995).
6. P. Di Trapani, A. Andreoni, P. Foggi, C. Solcia, R. Danielius, and A. Piskarskas, Opt. Commun. **119**, 327 (1995).
7. A. Baltuška, T. Fuji, and T. Kobayashi, Opt. Lett. **27**, 306 (2002).
8. P. Tzankov, J. Zheng, M. Mero, D. Polli, C. Manzoni, and G. Cerullo, Opt. Lett. **31**, 3629 (2006).
9. E. Riedle, M. Beutter, S. Lochbrunner, J. Piel, S. Schenkl, S. Spörlein, and W. Zinth, Appl. Phys. B **71**, 457 (2000).
10. T. Kobayashi and A. Baltuska, Meas. Sci. Technol. **13**, 1671 (2002).
11. D. Brida, C. Manzoni, G. Cirmi, M. Marangoni, S. Bonora, P. Villoresi, S. De Silvestri and G. Cerullo, J. Opt. **12**, 013001 (2010).
12. C. Manzoni and G. Cerullo, J. Opt. **18**, 103501 (2016).
13. M. K. Reed, M. K. Steiner-Shepard, and D. K. Negus, Opt. Lett. **19**, 1855 (1994).
14. A. Brodeur and S. L. Chin, J. Opt. Soc. Am. B. **16**, 637 (1999).
15. M. Bradler, P. Baum, and E. Riedle, Appl. Phys. B **97**, 561 (2009).
16. P. Baum, E. Riedle, M. Greve, and H. R. Telle, Opt. Lett. **30**, 2028 (2005).
17. T. Shin, J. W. Wolfson, S. W. Teitelbaum, M. Kandyla, and K. A. Nelson, Rev. Sci. Instrum. **85**, 083115 (2014).
18. J. Piel, E. Riedle, L. Gundlach, R. Ernstorfer, and R. Eichberger, Opt. Lett. **31**, 1289 (2006).
19. M. Zavelani-Rossi, D. Polli, G. Cerullo, S. De Silvestri, L. Gallmann, G. Steinmeyer, and U. Keller, Appl. Phys. B **74**, s245 (2002).
20. M. R. Armstrong, P. Plachta, E. A. Ponomarev and R. J. D. Miller, Opt. Lett. **26**, 1152 (2001).
21. R. Trebino, Frequency-Resolved Optical Gating: The Measurement of Ultrashort Laser Pulses (Springer US, 2000).
22. M. Bellini and T. W. Hänsch, Opt. Lett. **25**, 1049 (2000).
23. Z. Bor and B. Rácz, Opt. Commun **54**, 165 (1985).
24. C. Homann, N. Krebs, and E. Riedle, Appl. Phys. B **104**, 783 (2011).
25. M. Beutler, M. Ghotbi, F. Noack, D. Brida, C. Manzoni, and G. Cerullo, Opt. Lett. **34**, 710 (2009).
26. I. Z. Kozma, P. Baum, S. Lochbrunner, and E. Riedle, Opt. Express **11**, 3110 (2003).
27. U. Banin, A. Waldman, and S. Ruhman, J. Chem. Phys. **96**, 2416 (1992).
28. P. R. Poulin, Coherent Lattice and Molecular Dynamics in Ultrafast Single-Shot Spectroscopy (Massachusetts Institute of Technology, 2005).
29. P. R. Poulin and K. A. Nelson, Science **313**, 5794 (2006).